IOSR Journal of Applied Geology and Geophysics (IOSR-JAGG)
e-ISSN: 2321–0990, p-ISSN: 2321–0982.Volume 6, Issue 6 Ver. I (Nov. – Dec. 2018), PP 56-71
www.iosrjournals.org

Geodynamic Environment and Geochemical Control of Gabbroic Intrusions in Southwest Haut-Katanga in the Kapande Area: (Democratic Republic of Congo)

Mwitwa K.M[a] , Mwabanua M.C[a] , Kapajika B.C,Nkiko H.E[a] , Mashala T.P[a], , Mugisho.B.J[a] , Kasongo M. P [c], Twasakidila M. T.[a], Dash M. R. [b] , Sahoo H. K.[b]

[a] *Department of Geology, University of Lubumbashi, B.P.1825, Lubumbashi, Democratic Republic of Congo*
[b] *Department of Geology, Agora Metals SARL, Lubumbashi, Democratic Republic of Congo*
[c] *Department of Geology, University of Likasi, B .P 1946, D. R.Congo*
Corresponding Author: Mwitwa K.M

ABSTRACT
Continental intraplate volcanism is less expressed compared to other geodynamic frameworks. This volcanism is of obvious geodynamic interest because it is always related to the phenomena of rupture of the continental plates that can lead to the opening of the oceanic domains. The mapping and lithostratigraphy of the Kapande sector led to the development of geological sections that intercept basic intrusions of a gabbroic nature. The intrusive nature of these gabbros has been demonstrated by the existence of two facies, a fine border facies surrounding coarse facies in the heart of the intrusion. The petrographic examination of these rocks proves that they are characterized by a distinctly grainy texture with double-mic basic plagioclase, pyroxenes of monoclinic type, probably augite, opaque minerals and some spherical crystals and quartz observed. in one of the samples. The chemical composition is clearly basic with SiO_2 percentages ranging from 40.55 to 46.10%, those in MgO less than 7% and an Al_2O_3 / (CaO + K_2O + Na_2O) ratio lower than 1. These results, which testify the aluminous nature of these gabbros. The content by weight of Na_2O oxides averaging 3.5% on average, explains the alkaline character of these gabbros and the alkaline series is typical of the intra-continental plates. These findings result from the use of the discriminant diagram (Nb / Zr) vs Zr (Denis Thiéblemont & Monique Tégyey, 1994).

Keywords: *Pleated Katangan - gabbroic intrusions - continental intra-plate areas - Kapande*

Date of Submission: 26-11-2018 Date of acceptance: 10-12-2018

I. Introduction

Kapande is located in Haut-Katanga in the Southeast of the Democratic Republic of Congo. It represents our study area and is located near the Zambian border 30 km from the city of Kipushi.

Katanguien, all folded formations between 900 and ± 600 Ma and unaffected by folds earlier than 950 Ma, are called folds. They were folded around 950 Ma by the Lomamian orogeny, about 850 Ma by the Lusakian orogeny and around 600 Ma by the Lufilian orogeny. The last orogeny is the most important because it has impressed on the Upper Proterozoic rocks the arc pattern we are currently seeing (Ngoyi & Dejonghe, 1995, Kampunzu & Cailteux, 1999, Kampunzu, et al., 2000, Batumike, et al. 2007, Cailteux et al., 2007). There are two continuous tillites that have been deposited synchronously throughout the basin. The presence of these tillites made it possible to divide the Katangian into three groups. The Roan group, the Nguba group and the Kundelungu group can be distinguished from the bottom up (Table 1: François, (1973) (Cailteux et al., 1994) (Batumike et al., 2007). magmatic rocks found in the Katangian, were mainly established around 600 Ma (Demesmaeker et al, 1963) and are located singularly in the heart of the anticlinal structures, along zones of deep faults, or outcropping in the form of salaries. sporadic little extended.

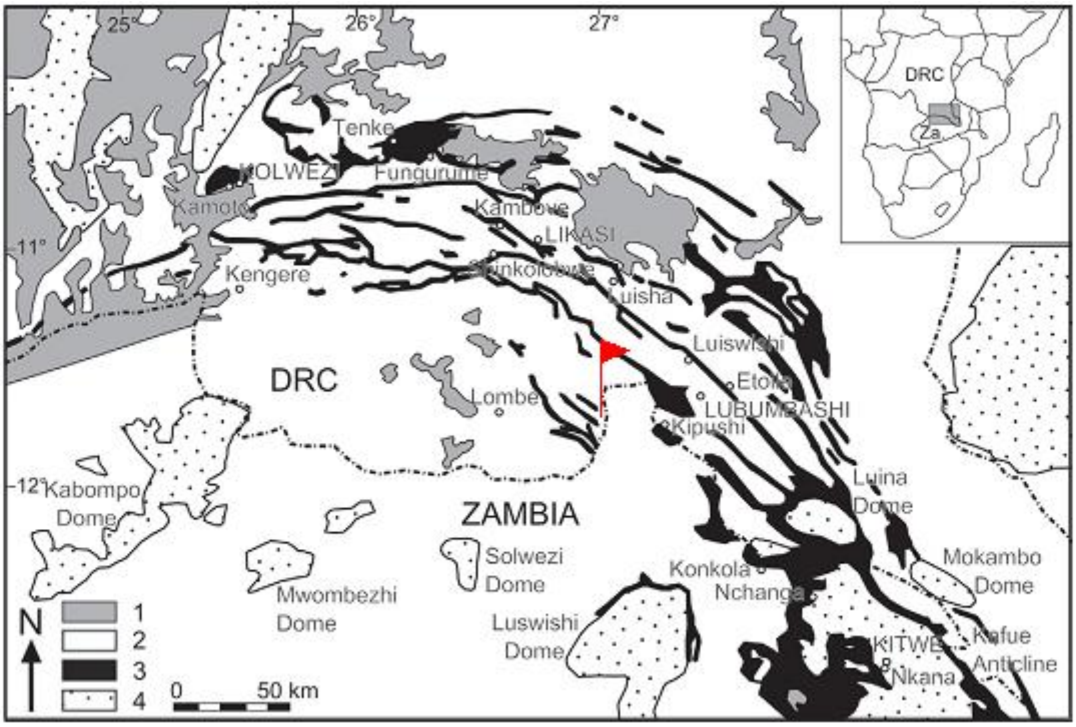

Fig. 1. Geological map of the Copperbelt of Central Africa with the location of important deposits. 1: Post-Katangian Rocks; 2: Mwashya, Nguba and Kundelungu Rocks; 3: Rifts, Breaches and Roan Rocks; 4: Pre-Katangian basement. According to François (1974).

The Copperbelt of Central Africa (Fig1) is one of the largest and richest metallogenic provinces in the world (Cailteux et al., 2005, Hitzman et al., 2005, Selley et al., 2005).

It stretches on the border between the Democratic Republic of Congo and Zambia, and is renowned for its deposits in Cu-Co. These metalliferous deposits are found in the Lufilian Arc (590-530 ma) and are most often the result of a multi-phase mineralization process (Cailteux et al, 2005, Dewaele et al, 2006, El Desouky et al. 2009, Hitzman et al., 2012, Selley et al., 2005).

As for pyroclastites, Lefebvre J. (1985) demonstrates that these volcanic products are syn-sedimentary. This study is part of a global research project on the geochemistry and petrology of gabbroic rocks in the Kapande region of southwestern Kipushi.

The objectives of this study can be summarized in three points:

• The mapping of these basic magmatic intrusions and the definition of the different facies that constitute them;
• The definition of the magmatic affinities of these rocks;
• Characterize and define the geodynamic context of their implementation.

II. Materials And Methodology

Basic geological material served a detailed field survey and laboratory studies were conducted on the samples. In order to carry out a complete field study, 56 samples were taken of which 15 were selected for the manufacture of thin sections in the Department of Geology of the University of Lubumbashi. The petrographic study was carried out using a transmitted light polarization microscope of brand ALLTION model NP-400 M and MOTIC PM-28 SERIES. For the geochemical study, 22 samples were selected and analyzed in major and trace elements. This study focused mainly on geochemical analyzes of magmatic rocks and aimed to determine the rock name according to the CIPW standard (Cross, Iddings, Pierason and Washington) as well as to highlight the generating magmatic series and the context geodynamics of setting up this this gabbroic intrusion. The analyzes were carried out for the major elements such as SiO2, TiO2, Al2O3, CaO, K2O, MgO, MnO, Na2O, P2O5, and FeO and trace elements, Co, Cu, Zn, Cr, Ni, V, Rb, Sr , Pb and Zr. All chemical analyzes were then processed through a set of software.

III. Results

3.1. LITHOSTRATIGRAPHY AND PETROGRAPHY

3.1.1. LITHOSTRATIGRAPHY

Field observations made it possible to place the Kapande rocks in the local geological context.

Profile 1

The first SSO - NNE oriented profile shows a gabbroic intrusion towards the south (Kibe - Kibe massif), hosted in dolomitic rocks. With the exception of this intrusive Kibe - Kibe massif, this profile highlights two alternating types of lithology including Shale and dolomite (Figure 2).

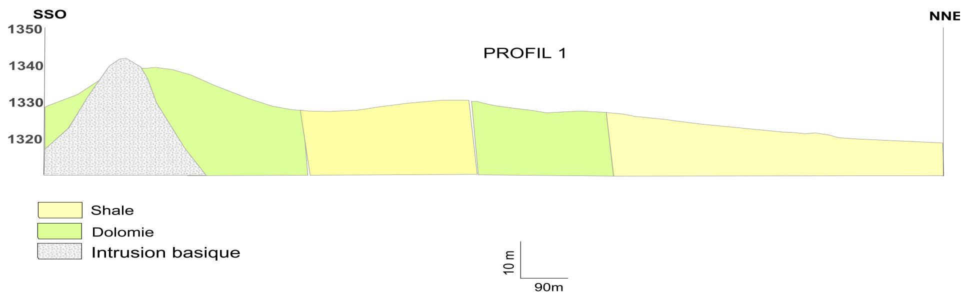

Profile 2

Oriented NE - SW, the second profile highlights an intrusive mass hosted in shales of brown color. The Kapande gabbroic massif, unlike the Kibe - Kibe outcrop, is less extensive and intrusive in shales (Figure 3).

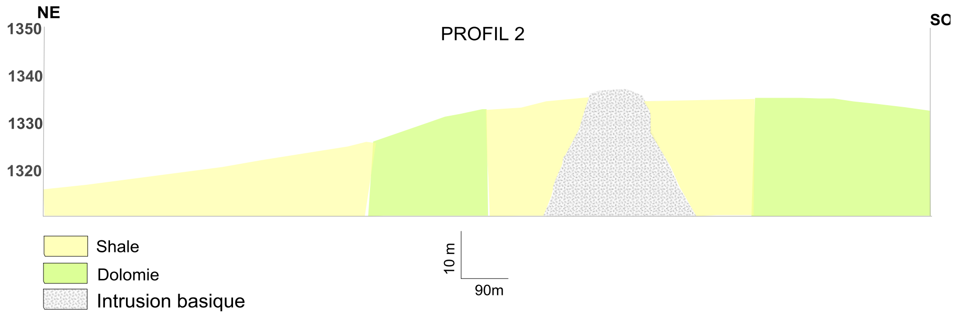

Profile 3

This profile intersects a red dolomitic formation in the south-west, intersected by a vast basic mass. It corresponds to the shortest profile of all (Figure 4).

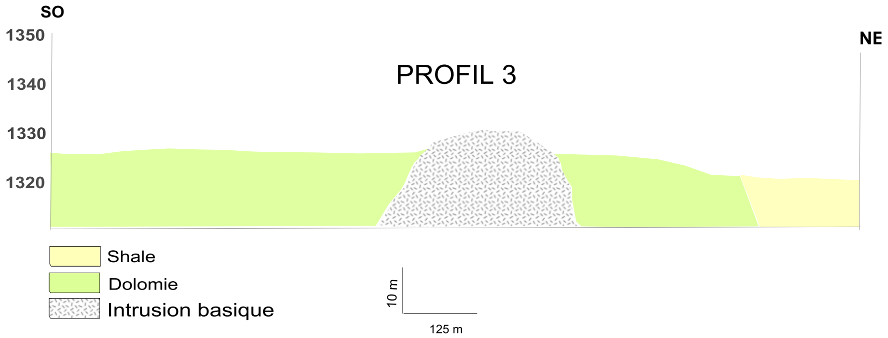

Profile 4

Direction SE - NO, this last profile intercepts two basic intrusive massifs (figure 5), the first mass is entered in a dolomite, more to the north outcrops the second mass which appears in turn within a clay formation.

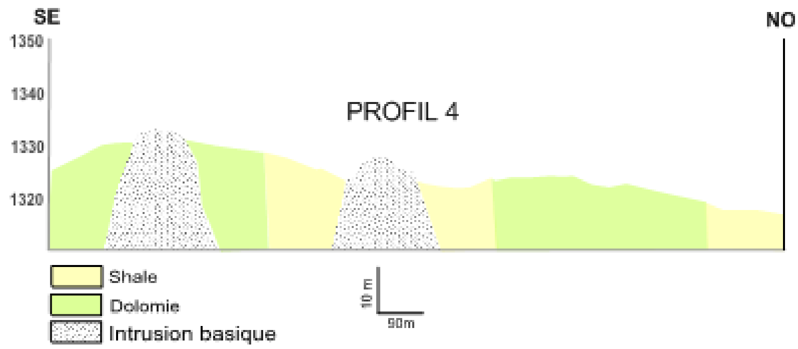

Two types of facies have been identified by the mapping study, one consisting of coarse crystal rock and the other of fine crystal rock. It is worth noting that the size of crystals increases from the border to the interior of the massif. In the coarse crystal zone, the size varies from 3 to 6 mm, but it ranges from 1 to 2 mm in the fine crystal zone. Figure 5 shows the facies Zonality of the Kibe-Kibe and Kapande Massif.

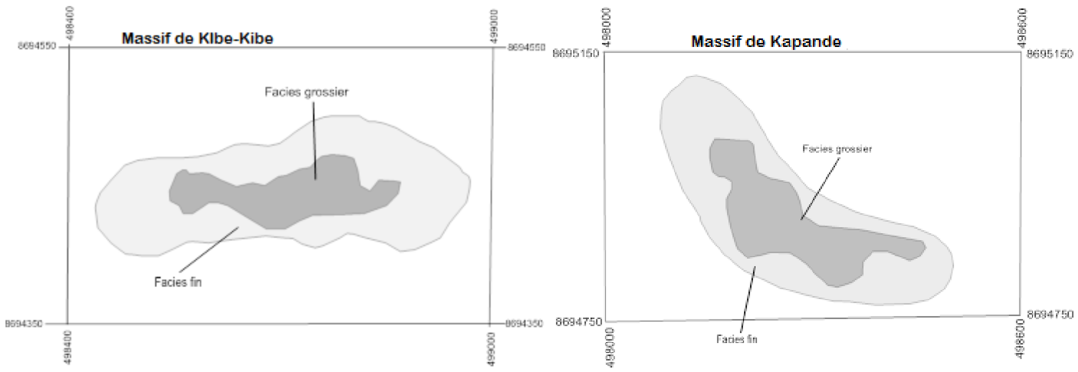

3.1.2. PETROGRAPHY

➢ **DESCRIPTION OF THE ROCKS OF THE COARSE FACES**

3.1.2.1 Description of the sample ed 1

Macroscopic view of ed1 Microscopic observation of ED1 (LPA on the left and LPNA on the right)

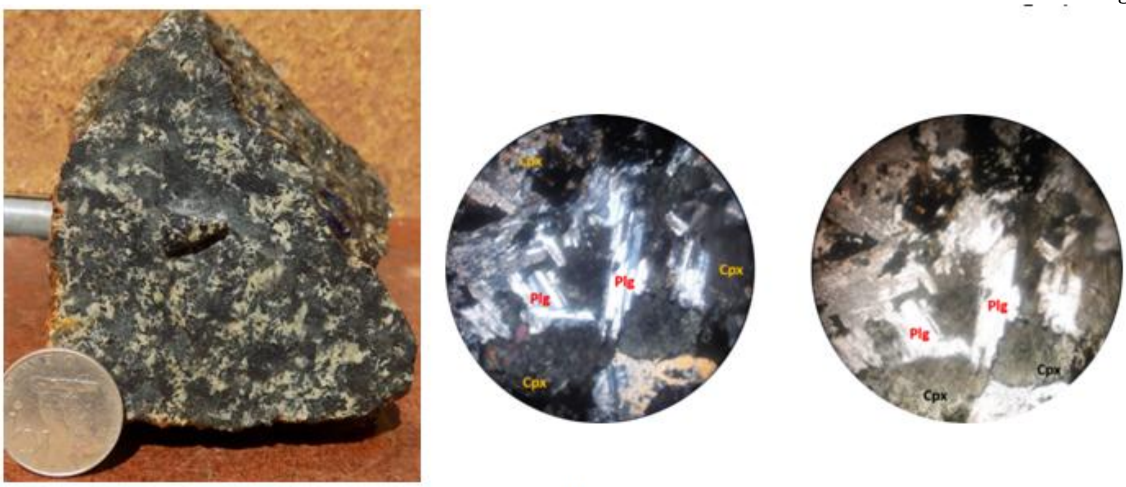

A B

Figure 7: A) Grainy-textured rock with dark coloration with plagioclase crystals ranging in size from 3-5 mm, the rock contains flake-laminated minerals, probably ferromagnesians. B) The ED1 slide has the following microscopic characteristics: Plagioclases (Plg) generally have a sub-automorphic morphology but are most often more automorphic and are in the form of rods. The size of the plagioclase grains is on average 1 mm

in the gabbros (s.s.), but it varies from 0.5 mm to 3 mm between the different samples and is relatively constant within the same sample. Plagioclases generally represent the most abundant phase with almost all modal proportions. The clinopyroxenes (Cpx) observed are generally in the form of sub-automorphic crystals. They often have inclusions of plagioclase, they are moderately altered with sometimes a reduction of the hue, which tends towards a rather dark color. The size of the clinopyroxene grains is on average about 1 mm but varies between 0.1 mm and 1.2 mm in the samples. Opaque minerals (Opq) are very rare in these rocks (≤ 1%) and are generally small. These minerals are mainly magnetites, ilmenites and sulphides. All opaque minerals have sub-automorphic to xenomorphic morphologies and are sometimes found in inclusion in plagioclase and clinopyroxene. Quartz (Qtz) appears on this preparation but has a very low proportion (<< 1%) The crystallization sequence is as follows: Plg - Cpx - Opq ± (Qtz)

Table 2- Syntheses on the observations of the ED1 sample

Sample Code	White Minerals	Colored Minerals	Minerals Accessories	Notes
ED1	Plagioclase Quartz	Clinopyroxene	Oxydes Sulphides	The rock is granular, the crystals of plagioclase and pyroxenes are sub automorphic. Note the very small presence of quartz crystals.

3.1.2.2 Description of the sampleED2

Macroscopic view of ED2 Microscopic observation of ED2 (LPA on the left and LPNA on the right)

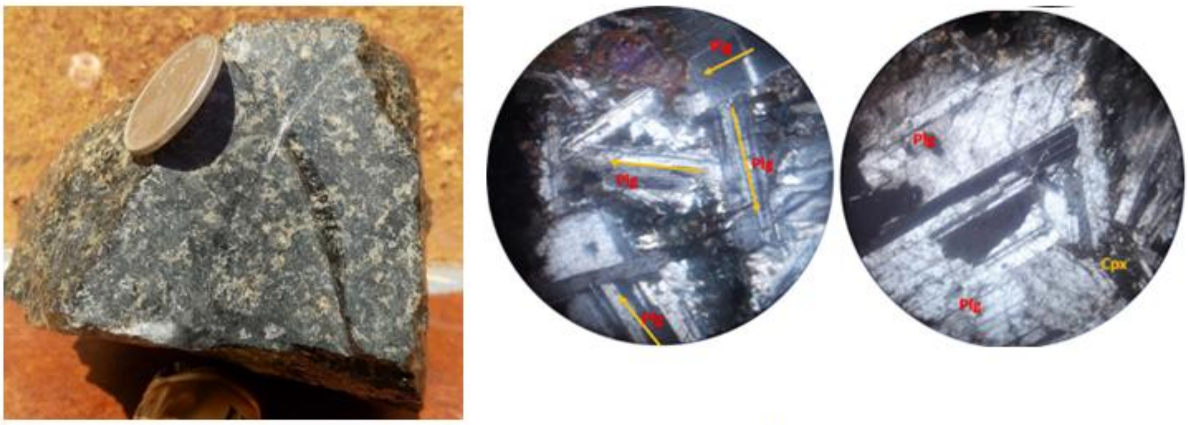

A B

Figure 8: A) Grosse-textured, dark-colored rock with very abundant plagioclase crystals (plagioclase) ranging in size from 4-6 mm, the rock contains flake-laminated minerals.B) The ED2 blade has the following characteristics: Microscopic Plagioclases show crystals that are automorphic to sub-automorphic, most of them lattice-shaped. These twin slats (Carlsbad and polysynthetic) have various orientations in the blade and therefore do not follow a preferred direction. Their size varies within the samples and is between 1 and 6mm. Clinopyroxenes are sub-automorphic or even interstitial; in most samples, clinopyroxenes are slightly altered. The size of the clinopyroxene grains is generally constant and varies on average from 0.5 mm to 3 mm. The opaque minerals observed in these gabbros are essentially oxides and sulphides, these minerals are sub-automorphic to xenomorphic and are sometimes observed in inclusions in pyroxenes. Opaque minerals are generally small (<0.3 mm) and scanty (≤ 2%). The textural relationships between the minerals in these gabbros make it possible to determine the following crystallization sequence: Plg - Cpx – Opq

Table 3- Syntheses on the observations of the ED2 sample.

Sample Code	White Minerals	Colored Minerals	Minerals Accessories	Notes
ED2	Plagioclase	Clinopyroxene	Oxydes Sulphides	The rock is granular, with plagioclases automorphic and large pyroxenes are sub-automorphic, speckled. Note the absence of quartz and the presence of an accessory mineral such as sphene

3.1.2.3 Description of the sample ED 10

Macroscopic view of ed10

Microscopic observation of ED10 (LPA on the left and LPNA on the right)

A

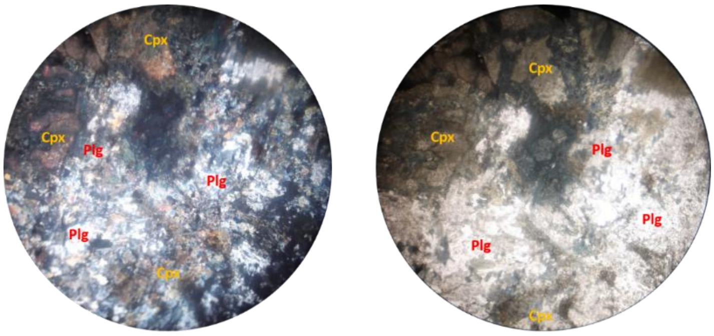

B

Figure 9: A) Dark-grained, textured rock with plagioclase size 3-6 mm, the rock contains bright laminated minerals.B) The ED10 slide, revealing some microscopic features compared to other samples: Altered Plagioclases are usually xenomorphic. In the studied slide, they are more abundant than the clinopyroxenes. The clinopyroxenes are observed mainly in xenomorphic crystals of variable size often including partially plagioclases. Like plagioclases, clinopyroxenes are also in the form of xenomorphic crystals. The opaque minerals, mainly iron oxides and sulphides, have a sub-automorphic to xenomorphic morphology. They are observed more rarely in inclusion in plagioclase or clinopyroxene. Opaque minerals are medium (≤ 0.2 mm) and generally not very abundant (<1% by volume). The textural relationships between the minerals in these gabbros make it possible to determine the following crystallization sequence: Plg - Cpx - Opq ± (Bt)

Table 4- Syntheses on observations of the ED10 slide.

Sample Code	White Minerals	Colored Minerals	Minerals Accessories	Notes
ED10	Plagioclase	Clinopyroxene Biotite	Oxydes Sulphides	Grosse-textured rock, whose plagioclase and pyroxene are clearly visible and automorphic. Presence of sphene and biotite.

➢ **DESCRIPTION OF THE ROCKS OF THE FIN FACIES**

3.1.2.4 Description of the sampleED 8

Macroscopic view of ED8

Microscopic observation of ED8 (LPA on the left and LPNA on the right)

A

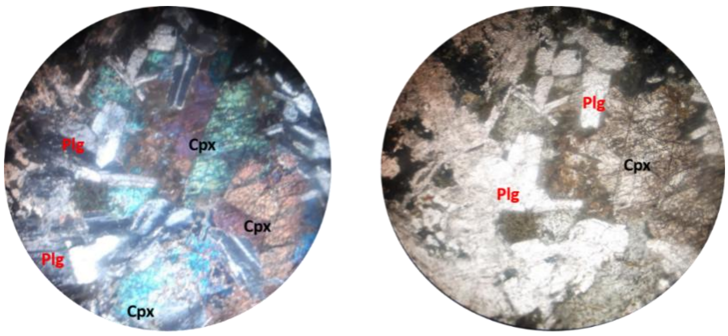

B

Figure 10: A) Rock rich in ferromagnesian minerals, dark color whose clear crystals represented by plagioclases become less visible in the matrix with a size less than 2mm. B) The microscopic description of this slide to demonstrate the following facts: The plagioclases are in the form of automorphic to sub-automorphic crystals and are partially bypassed by clinopyroxenes. No marks of remarkable alteration on this blade. Plagioclases generally have a larger crystal size of between 0.5 mm and 3 mm in all rocks. In the studied slide, they are more abundant than the clinopyroxenes. The clinopyroxenes are observed mainly in sub-automorphic to

xenomorphic crystals, sometimes twinned of variable size, surrounding the plagioclases. These morphologies are generally associated with smaller xenomorphic crystals situated in interstitial position between the other mineral phases.The opaque minerals observed would be iron oxides and sulphides. They are sub-automorphic to xenomorphic with an average size ≤ 0.2 mm and are generally scant <1% by volume. The textural relationships between the minerals in these gabbros make it possible to determine the following crystallization sequence: Plg - Cpx - Opq

Table 5- Syntheses on the observations of the sample ed8.

Sample Code	White Minerals	Colored Minerals	Minerals Accessories	Notes
ED8	Plagioclase	Clinopyroxene	Oxydes Sulphides	The rock is granular, with automorphic plagioclases and sub-automorphic pyroxenes. The pyroxenes are twinned and essentially in Carlsbad

3.2 GEOCHIMY
3.2.1 PRESENTATION OF DATA
3.2.1.1 MAJOR ELEMENTS

These elements, which account for more than 99% of the rock's chemical composition and have concentrations greater than 1% by weight in the geological materials, are listed in Table 6: Table 6 - Chemical analyzes in% of major elements

C	1	2	3	4	5	6	7	8	9	10	11
	ED14N	ED4N	ED8N	ED11N	ED21N	ED19N	ED24N	ED22N	ED9N	ED12N	ED13N
SiO_2	43,33	45,17	43,95	42,62	43,29	46,1	42,07	43,22	42,75	43,05	42,6
AL_2O_3	9,92	10,9	10,88	10,05	10,33	10,15	10,09	10,32	9,88	9,58	10,47
TIO_2	2,15	2,29	2,1	2,23	1,66	2,4	1,99	2,18	2,01	1,96	1,44
FEO	12,18	12,01	11,52	11,97	10,47	11,97	11,53	10,75	11,1	11,57	12,63
MGO	3,53	3,32	2,98	2,98	3,7	2,95	3,32	3,07	4,69	2,92	5,31
MNO	1,46	0,6	0,89	0,9	0,28	0,79	1,37	0,96	1,06	1,2	0,9
CAO	7,33	7,69	7,75	7,43	6,19	7,83	7,34	7,77	7,83	7,7	7,48
NA_2O	3,42	3,68	3,29	3,45	3,41	3,79	3,06	3,34	3,1	3,03	2,3
K_2O	0,72	0,68	0,56	0,54	0,7	0,41	0,62	0,52	0,38	0,69	0,25
P_2O_5	0,47	0,58	0,42	0,46	0,62	0,48	0,36	0,47	0,31	0,48	0,34
	12	13	14	15	16	17	18	19	20	21	22
	ED1C	ED15C	ED25C	ED7C	ED2C	ED27	ED30	ED3C	ED6C	ED23C	ED5C
SIO_2	44,51	40,99	43,76	42,9	41,9	43,76	45,85	40,55	41,29	41,72	41,12
AL_2O_3	9,35	9,54	9,43	8,96	11,05	12,57	11,66	10,22	9,62	10,45	11,09
TIO_2	1,94	1,83	2,19	1,82	1,68	2,17	1,8	1,86	1,84	1,89	2,03
FEO	13,2	11,6	13,42	13,22	9,4	9,4	8,92	11,57	13,32	12,54	11,02
MGO	3,98	3,47	2,82	3,4	3,35	3,13	3,33	3,42	3,28	3,52	2,94
MNO	1,26	0,83	1,09	1,44	1,44	1,73	1,27	1,09	0,86	1,15	0,99
CAO	7,32	6,61	6,39	6,75	8,01	8,03	8,52	6,82	6,62	6,39	6,95
NA_2O	3,05	2,81	3,49	2,88	2,61	3,38	2,77	2,91	2,94	3,03	3,13
K_2O	0,48	0,77	0,7	0,75	0,38	0,49	0,07	0,62	0,67	0,76	0,38
P_2O_5	0,43	0,44	0,48	0,38	0,45	0,32	0,41	0,51	0,57	0,53	0,55

3.2.1.2 TRACE ELEMENTS

These elements with contents below 0.1% were used to search for the origin of the magmas that produced the rocks observed. These contents of trace elements are expressed in ppm by mass of elements (Table 7).

Table 7: Chemical analysis in ppm of the trace elements

	1	2	3	4	5	6	7	8	9	10	11
	ED14N	**ED4N**	**ED8N**	**ED11N**	**ED21N**	**ED19N**	**ED24N**	**ED22N**	**ED9N**	**ED12N**	**ED13N**
Cu	252	238	329	262	249	316	274	243	281	282	170
Zn	94	101	156	137	92	126	104	124	46	93	87
V	221	207	334	299	196	326	365	308	226	330	280
Cr	68	97	0	0	103	0	91	0	155	0	146
Ni	62	63	5	57	50	58	75	57	132	67	115
Pb	7	12	0	11	8	17	0	12	0	7	0
Sr	369	371	363	368	345	361	361	367	323	366	418
Rb	28	26	29	30	23	21	30	27	21	26	28
Ta	255	246	258	260	259	244	251	249	207	280	209
Nb	60	64	40	53	39	57	37	50	42	41	20
Zr	205	210	155	170	120	191	124	184	112	173	101
	12	**13**	**14**	**15**	**16**	**17**	**18**	**19**	**20**	**21**	**22**
	ED1C	**ED15C**	**ED25C**	**ED7C**	**ED2C**	**ED27**	**ED30**	**ED3C**	**ED6C**	**ED23C**	**ED5C**
CU	246	341	342	361	190	356	268	281	300	358	257
ZN	72	36	43	104	100	86	64	49	136	36	91
V	289	255	344	291	231	299	317	309	257	394	232
CR	0	86	66	89	0	0	0	0	0	0	0
NI	69	87	62	85	65	63	65	79	52	88	65
PB	0	0	0	11	13	0	7	0	8	0	0
SR	279	318	307	306	361	404	406	314	358	327	350
RB	18	31	33	34	20	24	14	28	30	30	14
TA	249	273	241	192	261	289	277	226	260	233	273
NB	48	49	65	51	36	29	47	49	87	61	61
ZR	139	183	167	165	163	119	154	186	213	186	178

NORMATIVE CALCULATIONS

Table 8 - Mineral Distribution as Calculated by the CIPW Standard

	ED14N	**ED4N**	**ED8N**	**ED11N**	**ED21N**	**ED19N**	**ED24N**	**ED22N**	**ED9N**	**ED12N**	**ED13N**
APATITE	1.5	1.8	1.30	1.52	1.94	1.53	1.12	1.53	0.92	2.10	0.83
ILMÉNITE	5.80	6.24	5.64	6.39	4.54	6.67	0.97	6.16	5.19	5.18	3.03
ORTHOSE	6.04	5.76	4.65	4.78	5.96	3.54	5.18	4.57	3.07	5.69	1.64
ALBITE	13.62	16.13	18.73	15.55	15.49	13.87	16.98	17.27	16.19	14.56	19.35
DIOPSIDE	29.12	28.8	27.41	30.72	19.78	33.27	27.10	30.66	28.76	28.17	16.41
HYPERSTHÈNE	13.86	20.77	32.88	18.28	46.91	36.46	19.85	30.21	22.84	41.07	50.79
OLIVINE	30.06	20.45	9.38	22.73	5.36	4.63	28.66	9.63	23.03	3.21	7.94
	ED1C	**ED15C**	**ED25C**	**ED7C**	**ED2C**	**ED27**	**ED30**	**ED3C**	**ED6C**	**ED23C**	**ED5C**
APATITE	1.16	1.33	1.46	1.07	2.42	1.02	1.34	1.54	1.66	1.54	1.73
ILMÉNITE	4.62	4.79	5.86	4.47	7.86	5.95	6.76	4.92	4.68	4.77	5.52
ORTHOSE	3.54	6.31	5.87	5.74	5.51	4.21	6.17	5.11	5.33	5.98	3.19
ALBITE	12.97	15.32	11.23	12.01	42.7	25.48	25.86	18.02	14.82	16.77	21.62
DIOPSIDE	24.96	22.39	25.39	24.79	41.45	24.93	28.98	21	21.17	18.04	19.76
HYPERSTHÈNE	44.45	38.78	34.98	41.95	0	20.74	21.15	29.32	33.24	30.15	36.65
OLIVINE	8.29	11.78	15.19	10.46	0	17.66	9.74	19.88	19.09	22.71	11.51

CLASSIFICATION OF STRECKEISEN (1976)

This classification places the different samples of Kapande magmatic rocks in the family of gabbroic rocks (Figure 9) rich in plagioclase-type feldspar (P) and representing largely low proportions of quartz.

Table 9: QAP standard

	ED14N	ED4N	ED8N	ED11N	ED21N	ED19N	ED24N	ED22N	ED9N	ED12N	ED13N
Q	0	0	0	0	0	0	0	0	0	0	0
A	30,74	26,34	19,89	23,54	27,8	20.33	23,4	20,94	15,95	28,11	7,83
P	96,26	73,66	80,11	76,46	72,2	79.67	76,6	79,06	84,05	71,89	92,17
	ED1C	**ED15C**	**ED25C**	**ED7C**	**ED2C**	**ED27**	**ED30**	**ED3C**	**ED6C**	**ED23C**	**ED5C**
Q	0	0	0	0	0	0	0	0	0	0	0
A	21,46	29,6	34,34	32,34	11,42	14,19	17,34	22,09	26,46	26,3	12,87
P	78,54	70,84	65,66	67,66	88,98	85,81	82,66	77,91	73,54	73,7	87,13

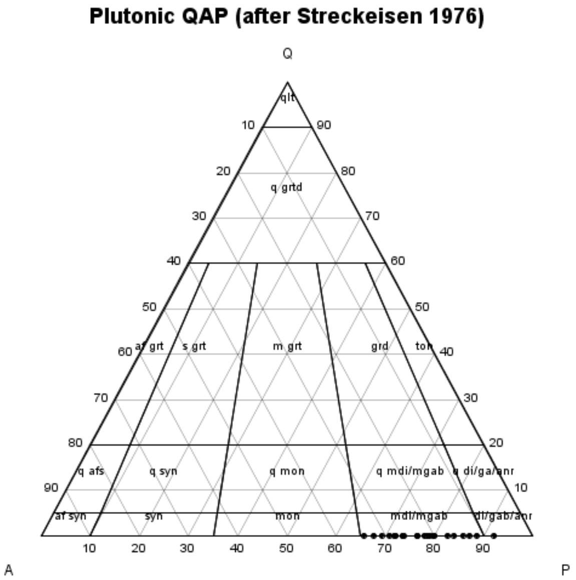

Figure 13 - QAP numeric fields (Streckeisen, 1976)

q mdi / mgab: Monzodiorite quartz and Monzogabbro; mdi / mgab: Monzodiorite and Monzogabbro; q di / gab: Quartz Diorite or Quartz Gabbro

TAS CHART (TOTAL ALKALIS-SILICA)

The SAR chart is one of the most used for magmatic rocks. The use of this diagram has been proposed by Cox et al. (1979) who demonstrated the importance of choosing SiO2 and Na2O + K2O as bases for a classification of magmatic rocks (Figure 14). This diagram distinguishes ultrabasic, basic, intermediate, and acidic rocks based on their silica compositions.

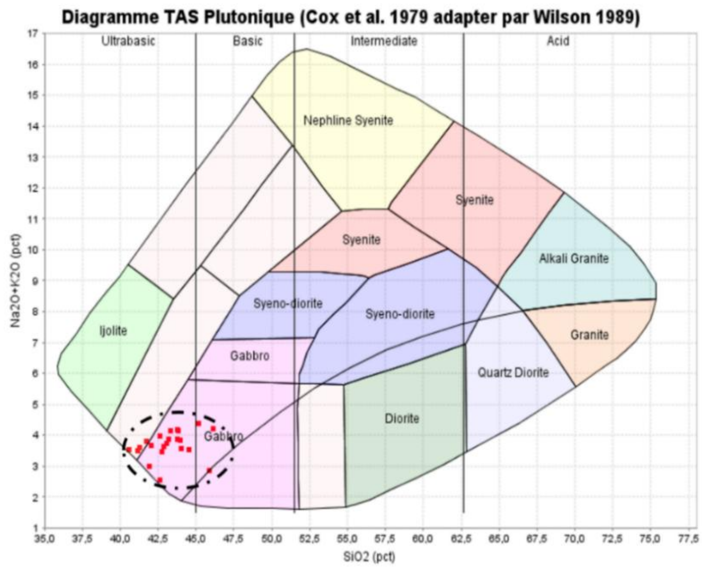

Figure 14 - TAS Plutonic Rock Chart (Cox et al., 1979, Wilson 1989)

The diagram in Figure 15 shows that all our samples are in the field of sodium alkaline gabbros.

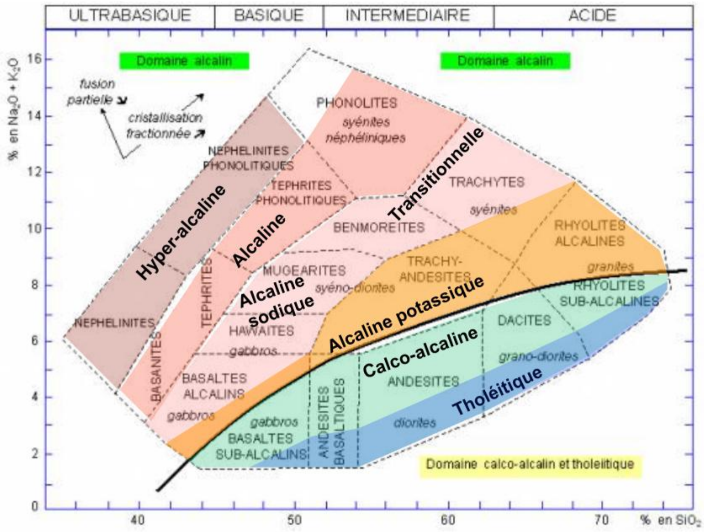

Figure 15 - TAS graph of plutonic rocks with magmatic series boundaries.

DIFFERENTIATION INDEX (D.I.)

It is an index that is calculated from the CIPW standard. It was introduced by Thornton and Tuttle (1960) for granites, but is now used for all magmatic rocks; it is supposed to express the ratio of white minerals in the rock, from the calculation of the weight percentages of the light-colored minerals of the standard (Table 10). So : $\boldsymbol{D.I = Qz + Or + Ab + Ne}$ Where Gold is orthoclase, Ab is albite and Ne is nepheline.

The differentiation index generally remains below 35% for an undifferentiated primary magma (Kabengele, 1986).

TABLE 10: DIFFERENTIATION INDICES (WEIGHT TABLE)

	ED14N	ED4N	ED8N	ED11N	ED21N	ED19N	ED24N	ED22N	ED9N	ED12N	ED13N
QUARTZ	0	0	0	0	0	0	0	0	0	0	0
ORTHOSE	6,04	5,76	4,65	4,78	5,96	3,54	5,18	4,57	3,07	5,69	1,64
ALBITE	13,62	16,13	18,73	15,55	15,49	13,87	16,98	17,27	16,19	14,56	19,35
NÉPHÉLINE	0	0	0	0	0	0	0	0	0	0	0
I.D	**19,66**	**21,89**	**23,38**	**20,33**	**21,45**	**17,41**	**22,16**	**21,84**	**19,26**	**20,25**	**20,99**
	ED1C	**ED15C**	**ED25C**	**ED7C**	**ED2C**	**ED27**	**ED30**	**ED3C**	**ED6C**	**ED23C**	**ED5C**
QUARTZ	0	0	0	0	0	0	0	0	0	0	0
ORTHOSE	3,54	6,31	5,87	5,74	5,51	4,21	6,17	5,11	5,33	5,98	3,19
ALBITE	12,97	15,32	11,23	12,01	42,7	25,48	25,86	18,02	14,82	16,77	21,62
NÉPHÉLINE	0	0	0	0	0	0	0	0	0	0	0
I.D	**16,51**	**21,63**	**17,1**	**17,75**	**48,21**	**29,69**	**32,03**	**23,13**	**20,15**	**22,75**	**24,81**

Our samples mainly have a differentiation index of less than 35%, this shows us that we are dealing with a primary origin (undifferentiated) of our generator magma.

ALTERATION INDEX AND HYPER-ALUMINOSITY INDEX

Alteration indices (Table 11) AI = [MgO + K2O / MgO + K2O + CaO + Na2O] × 100 and hyper-aluminosity (Table 12) PI = [Al2Omol / (CaOmol + Na2Omol + K2Omol)], provide good information on the intensity of the alteration affecting the magmatic rocks.

It should be noted that the mean values of the A.I. index of the mid-oceanic wrinkle basalts (MORB) and the unaltered arcuate basalts (VAB) are respectively 36 ± 8 and 34 ± 10; (LaFleche et al., 1991). Note that chloritization and sericitization of mafic rocks lead to A.I values. greater than 50 while the albitization causes a decrease of this index under the threshold of 30.

Table 11 - Alteration Rates in Samples

	ED14N	ED4N	ED8N	ED11N	ED21N	ED19N	ED24N	ED22N	ED9N	ED12N	ED13N
I.A	28,37	26,02	24,29	24,46	30	22,4	27,44	24,42	31,72	25,19	36,23
	ED1C	ED15C	ED25C	ED7C	ED2C	ED27	ED30	ED3C	ED6C	ED23C	ED5C
I.A	30,08	31,03	26,28	30,11	26	24,1	23,18	29,33	29,28	31,2	24,75

In the case of mafic rocks, an index of P.I. greater than 1 indicates a relative leaching of alkalis with respect to alumina. High values of the P.I. index generally involve hydrothermal leaching of the alkalis. Note that no sample gave a value of P.I greater than 1.

Table 12 - Rates of Hyperaluminosity Index in Samples

	ED14 N	ED4N	ED8N	ED11 N	ED21 N	ED19 N	ED24 N	ED22 N	ED9 N	ED12 N	ED13N
I. P	0,5	0,52	0,54	0,51	0,55	0,48	0,53	0,51	0,5	0,48	0,59
	ED1C	ED15 C	ED25 C	ED7C	ED2C	ED27	ED30	ED3C	ED6C	ED23 C	ED5C
I. P	0,5	0,55	0,52	0,5	0,57	0,61	0,58	0,57	0,55	0,6	0,61

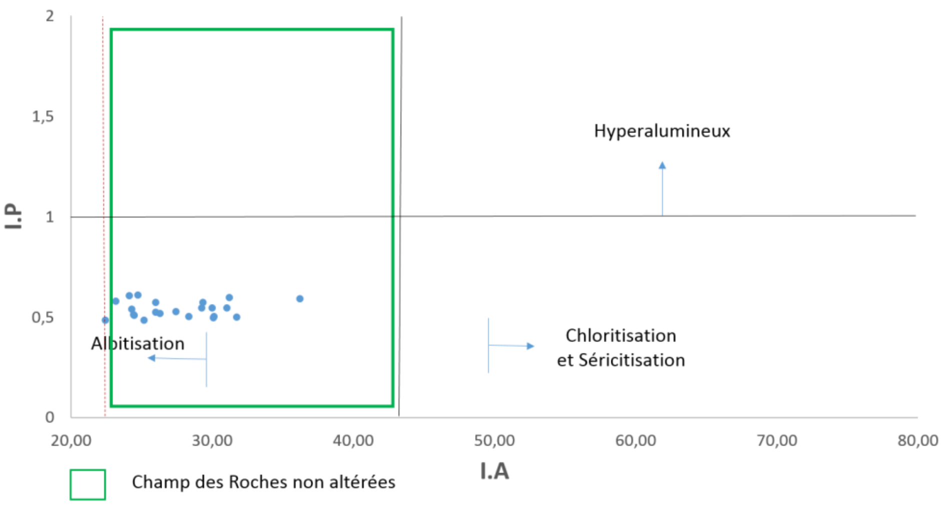

Figure 16 - Diagrams of the index of hyper-aluminosity (PI.) According to the index of deterioration (A.I.). At first glance, these observations suggest that samples of mafic rocks visually selected as fresh did not undergo significant hydrothermal alteration.

MAGMATIC AFFINITY

Modern petrology distinguishes three main types of magmatic series: alkaline, tholeiitic and calc-alkaline. The Na2O + K2O vs. SiO2 diagram (Irvine & Baragar, 1971), frequently used to separate alkaline and sub-alkaline rocks, also shows that almost all of the samples in our study area are in the alkaline range (Figure 17). The subalcaline domain is divided into calco-alkaline and tholeiitic series, the latter being richer in iron than the former.

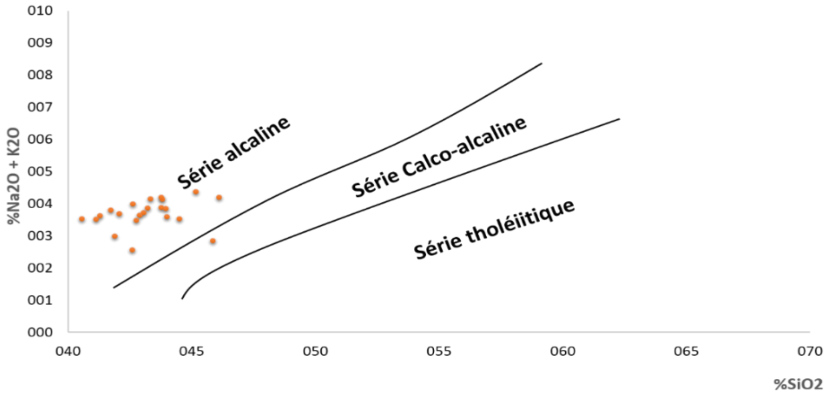

Figure 17 - Classification chart of a magmatic series

GEODYNAMIC CONTEXT OF THE SETTING

Pearce et al. (1984) defined the different geodynamic contexts of magma emplacement using a diagram based on the variation of the zirconium content (Zr) with respect to the niobium content on zirconium multiplied by the number of samples (n = 22 for our case): (Nb / Zr) N-Zr (Figure 18 and Table 13).

The result of this study (diagram in Figure 18) shows the gabbroic rocks flush in the Kapande area mainly related to an intra-plate alkaline magmatism.

However, a minority of points fall into the domain corresponding to the magmatism of the collision zones. This could be due to the fact that the mantle basaltic magma was mixed with the overlying crustal material during its ascent. As a result, some of these rocks have inherited the crustal geochemical signature (fgure19)

Table 13 - Discrimination Table of the Geodynamic Context of Magmatism

	ED14 N	ED4N	ED8N	ED11 N	ED21 N	ED19 N	ED24 N	ED22 N	ED9 N	ED12 N	ED13 N
(Nb/Zr)*n	6,44	6,7	5,68	6,86	7,15	6,57	6,56	5,98	8,25	5,21	4,36
Zr (ppm)	205	210	155	170	120	191	124	184	112	173	101
	ED1C	ED15 C	ED25 C	ED7C	ED2C	ED27	ED30	ED3C	ED6 C	ED23 C	ED5C
(Nb/Zr)*n	7,6	5,89	8,56	6,8	4,86	5,36	6,71	5,8	8,99	7,22	7,54
Zr (ppm)	139	183	167	165	163	119	154	186	213	186	178

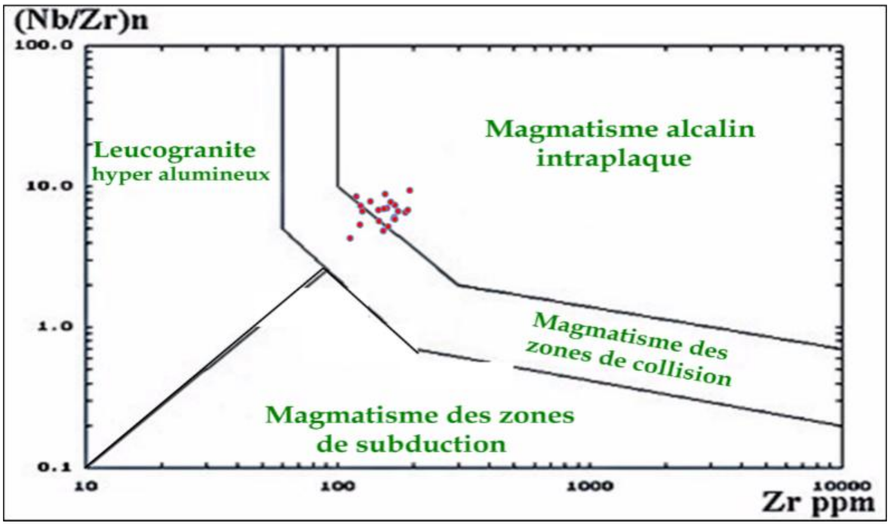

Figure 18 - Diagram of discrimination of the geodynamic context as a function of (Nb / Zr) * Zr Vs Zr. According to thieblemnt & Tégyey, 1994

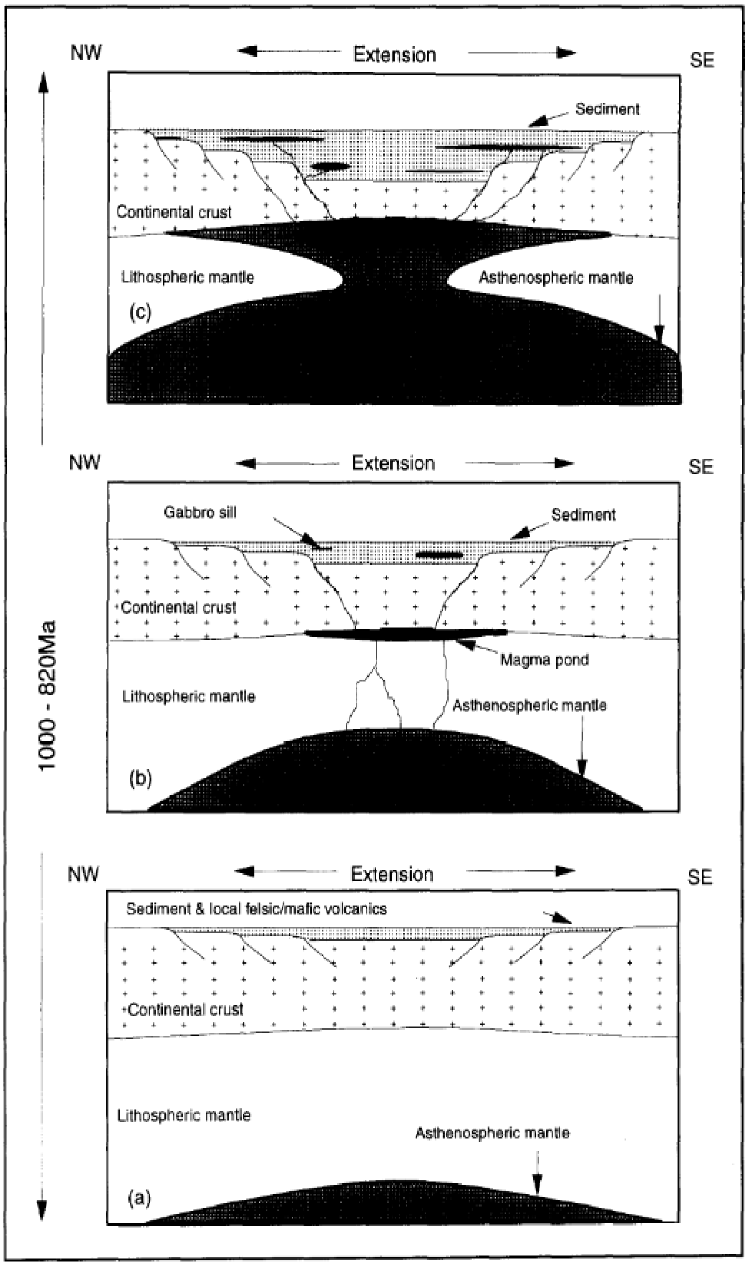

Figure 19 : schematic diagram showing three stages of the possible evolution of the Katangan Basin. (a) An early stage of initial rifting. (b) an intermediate stage of early mafic magmatism. (c) a late stage of rupture and less enriched mafic magmatism.

IV. Discussion And Conclusion

The Neoproterozoic formations constituting the Copperbelt have deposited in an intra-cratonic basin linked to a pan-African continental rift, probably about 400 kilometers long (Kampunzu and Cailteux 1999, Porada and Berhorst 2000). The 1 to 3 kilometer thick sediments that have filled this basin, now called the Roan Supergroup, have been deposited in carbonate and clasticstone cycles whose thickness and facies have changed over time (Lefebvre, 1989a, Cailteux et al. 1994, Hitzman et al., 2005). Several faults and extensional fractures have enlarged the basin in which they have formed new lands (Unrug 1988, Porada and Berhorst 2000), and these have been named Nguba Supergroup (Lower Kundelungu) and Kundelungu (Upper Kundelungu) before the rifting movement stopped around 573 Ma (Kampunzu and Cailteux, 1999, Master et al., 2005).

According to Oosterbosch 1959, Lefebvre 1973 and 1975, Mashala 2007, the magmatic rocks that are observed in the Katangian would have developed around 600 Ma. Lefebvre (1973) states that the Katangian has undergone significant essentially basic magmatic phenomena by studying the pyroclastic rocks of the lower Mwashya. The magmatic rocks observed in the Katanguian are located in the following 5 levels: (1) the Sub-Group of Mines where we have basic rocks replacing the Argilo-Mossy Gray Rock in the Etoile deposit

(Cailteux, 1994)), in the sector of Kambove (Cailteux, 1983, 1994) and in the mining polygon of Lwishya in the same stratigraphic level (Lefebvre and Cailteux, 1975). Cluzel (1986) also observes such rocks in close relationship with the dolomitic ensemble of the Kambove Formation (CMN). (2) In Dipeta there are sills and dykes of intrusive gabbroic and doleritic rocks at Mwadingusha and Kankonge (Oosterbosch, 1959, Lefebvre, 1975) and those of andesites more or less spilitized at Makawe, Shinkolobwe and Kipushi, respectively. (3) In the Mwashya below Kipoi, Kapolowe and especially Shituru (Likasi). Lefebvre (1973) reports the presence of the basic pyroclastic levels formerly known as "Kipoi breaches" in the localities of Kipoi, Kapolowe, Kompina, Mulungwishi, Gombela, and Shituru Quarry. These rocks, which have varied aspects ranging from true tuffs and lapilli, to argillites, have also been recognized in the Kambove sector of Kamoya (Cailteux, 1983, Mashala, 2007) under their beryllic facies only. (4) Cailteux et al. 2003 noted the presence of this type of rocks at Lwiswishi; in the big conglomerate of the Nguba Sub - Group where we have basic lava. (5) Doleras are reported in Kundelungu where gabbro dykes are found in Kalolo, Moba (Kapenda, 1986). As for the deposits of the Sub-Group of Mines, the small extension, the discreet and sporadic character of the volcanic products recognized just at the base and sporadically at the top of the series and the enormous volume of the mineralization observed in this group make it certainly less obvious. this relationship (Okitaudji, 1989 and 1997, Loris, 1996). The purpose of this paper was to determine the petrographic characteristics and geochemical variations of the basic Kapande plutonic rocks.

Mapping and lithostratigraphy have resulted in the development of geological sections that intercept basic intrusions. The stratigraphy of the observed terrains shows that they are formations of the Nguba group, characterized by an alternation of shales and dolomites. This succession has been specified by a study of the physicochemical characteristics of the soils and termite mounds that form there. Basic intrusions are characterized in landscape by a morphology of small massifs or rounded blocks. The intrusiveness of these intrusions has been demonstrated by the existence of two facies, a fine border facies surrounding a coarse facies at the heart of the intrusion. From a petrographic point of view, these rocks are characterized by a distinctly granular texture whose order of crystallization ranges from basic double-bonded plagioclase, to quartz passing respectively by pyroxene of monoclinic type probably augite, opaque minerals and some sphene crystals. These minerals observed in particular by Tembo et al. (1999) make up the gabbros described by them. These gabbros are considered to be the result of basaltic magmas with a chemical signature relating to intraplate magmatism.

Geochemically, the chemical composition is clearly basic with SiO2 contents ranging from 40.55 to 46.10%, MgO less than 7% and the average sum Fe + Mg + Mn + Ti is 18.

These gabbros whose ratios Al2O3 / (CaO + K2O + Na2O) are less than 1, which attests their aluminous nature.

The primary and undifferentiated character of the magma is indicated by the generally less than 35 value of the differentiation index.

In the alkali-silicate diagram of Irvine and Baragar (1971), Kapande gabbros are placed in the field of alkaline rocks. They show generally high levels of Cu, V, Sr, and Zr and relatively low in Cr, Zr, Co, Rb and Ni.

The Rb / Sr ratio varies according to the outcrops, the majority of outcrops have values between 0.07-0.11 which are closer to the mantle values (0.01-0.02 for the dorsal basalts) (Leroy, 1978).

Using the geochemical and geotectonic discrimination diagram [(Nb / Zr) xn] / Zr of Thiéblemont & Tégyey (1994), our samples fall into the field of "intra-alkaline magmatism". The granitoids related to this type of magmatism are probably the only ones to be correctly classified based solely on their geochemistry, with granitoids from other geodynamic contexts requiring additional dating and geological observations in addition (Forster et al., 1997).

References

[1]. BATUMIKE, M., CAILTEUX, J., & KAMPUNZU, A. (2007). Lithostratigraphy, basin development, base metal deposits, and regional correlations of the Neoproterozoic Nguba and Kundelungu rock successions, central African Copperbelt. Gondwana

[2]. CAHEN, L. (1954). La Géologie du Congo Belge. Liège: Vaillant-Carmanne.

[3]. CAHEN, L., & MORTELMANS, G. (1940). Contribution à la carte géologique du Katanga. La géologie des degrés carrés de Mokabe Kasari et Sampwe. In : Bulletin de la Société Belge de Géologie, de Paléontologie et d"Hydrologie, 50, 6-47.

[4]. CAILTEUX, J., 1983. Le Roan shabien dans la région de Kambove (Shaba-Zaïre). Etudes sédimentologique et métallogenique. Doctorate Thesis, University of Liege, Belgium, p. 232.

[5]. CAILTEUX, J. (1994). Lithostratugraphy of the neoproterozoic Shaba-type (Zaïre) Roan Super-Group metallogenisis of associated mineralization.

[6]. CAILTEUX, J. (2003). Proterozoic sediment-hosted base metal deposit of western Gondwana. 3 rd Conference and Field Workshop. Lubumbashi.

[7]. CAILTEUX J., Kampunzu A., Lerouge C., Kaputo A., Milesi J.P. (2005): Genesis of sediment-hosted stratiform copper-cobalt deposits, central African Copperbelt. Journal of African Earth Sciences 42, pp 134-158.

[8]. CAILTEUX, J., KAMPUNZU, A., & LEROUGE, C. (2007). The Neoproterozoic Mwashya-Kansuki sedimentary rock succession in the Central African Copperbelt, its Cu-Co mineralization, and regional correlations. Gondwana Research, 414-431.

[9]. CLUZEL, D., 1986: Contribution à l'étude du métamorphisme des gisements cupro-cobaltifères stratiformes du Sud-Shaba, Zaïre. Le district minier de Lwishia: Journal of African Earth. Sciences, vol. 5, no. 6, p. 557-574.

[10]. DEMESMAEKER, G., FRANCOIS, A., & OOSTERBOSCH, R. (1963). Gisements stratiformes de cuivre en Afrique. In : J.Lombard et P.Micolini, 2ème partie. Association de services Géologiques Africaines, 47-115.

[11]. DEWAELE S, MUCHEZ P, VETS J, FERNANDEZ-ALONZO M, TACK L (2006): Multiphase origin of the Cu-Co ore deposits in the western part of the Lufilian fold-and-thrust belt, Katanga (Democratic Republic of Congo). J Afr Earth Sci 46:455–469

[12]. EL DESOUKY HA, MUCHEZ P, CAILTEUX J (2009) Two Cu-Co sulfide phases and contrasting fluid systems in the Katanga Copperbelt. Democratic Republic of Congo: Ore Geology Reviews 36:315–332

[13]. FRANCOIS , A. (1987). Synthèse géologique sur l'arc du Shaba (Rép.du Zaïre) Centenaire de societe Belge de Géologie,These.

[14]. FRANCOIS , A. (2006). La partie centrale de l‟Arc cuprifère du Katanga : étude géologique. Tervuren African Geoscience collection, Vol. 109,61.

[15]. FRANCOIS, A. (1973). L‟extrémité occidentale de l‟arc cuprifère shabien. Etude géologique. Likasi, Zaïre. 113 p

[16]. FRANCOIS, A. (1987). Synthèse géologique sur l‟arc cuprifère du Shaba (Rép. Du Zaïre). Centenaire de la Société Belge de Géologie15-65

[17]. FRANCOIS, A. (1995).Problème relatifs au Katanguien du Shaba.Musée Royal de l'Afrique Centrale, Tervuren (Belgique). Annales des Sciences Géologiques. 101, 1 -20.

[18]. GYSIN, M. (1934). Les roches éruptives basiques de la Haute Lufira (Congo belge). Comptes rendus des séances de la société de physique et d‟histoire naturelle de Genève, 210-213.Geneve.

[19]. HITZMAN MW, KIRKHAM R, BROUGHTON D, THORSON J, SELLEY D (2005)The sediment-hosted stratiform copper ore system. In: Hedenquist JW, Thompson JFH, Goldfarb RJ, Richards JP (eds.) Economic Geology 100th Anniversary Volume, pp. 609–642

[20]. HITZMAN, M.W., BROUGHTON, D., SELLEY, D., WOODHEAD, J., WOOD, D., BULL, S., 2012. The Central African Copperbelt: Diverse Stratigraphic, Structural, and Temporal Settings the World's Largest Sedimentary Copper District. In: Society of Economic Geologists Special Publication 16, pp. 487e514.

[21]. INTIOMALE, M. (1982). Le gisement de Pb, Zn, Cu de Kipushi (Shaba-Zaïre). Thèse de doctorat. Université catholique de Louvain. Louvain, Belgique.

[22]. IRVINE, T., & BARAGAR, W. (1971). Aguide to the chemical classification of the common volcanic rocks. Revue canadienne des Sciences de la Terre, 523-548.

[23]. JACKSON, M., WARIN, O., WOAD, G., & HUDEC, M. (2003). Neoproterozoic allochtonous salt tectonics during the Lufilian orogeny in the Katangan Coppert, central Africa. Geological Society of America Bulletin, 314-330.

[24]. KABENGELE, M. (1986). Magmatisme Ubendien de PEPA-LUBUMBA sur le plateau des MARUNGU (Nord-est du Shaba, Zaïre). Etudes structurale, pétrologique, géochimique et signification géodynamique. Thèse de doctorat, UNILU. Vol I. 323p. Lubumbashi.

[25]. KALAMBA, T., KHONDE, M., ILUNGA, N., & MANSINSA, M. (1998). Monographie de la Province du Katanga. PNUD/UNOPS. Programme national de relance du secteur agricole et rural (PNSAR), p 137.

[26]. KAMPUNZU, A., & CAILTEUX, J. (1993). Lithostratigraphy of the Neoproterozoic Shaba type (Zaire) Roan supergroup and metallogenisis of associated stratiform, mineralization. Afrique Earth Science, 19,41,279-301.

[27]. KAMPUNZU, A., & CAILTEUX, J. (1999). Tectonic Evolution of the Lufilian Arc (Central Africa Copper Belt) During Neoproterozoic Pan African Orogenesis. Gondwana Research, 2, 401-421.

[28]. KAMPUNZU, A., TEMBO, F., KAPENDA, D., & HUNTSMAN. (2000). Neoproterozoic Katangan Basin, Central Africa: Implications for Rodinia Break-up. Gondwana Research, 125-153.

[29]. KAMPUNZU, A., TEMBO, F., MATHEIS, G., KAPENDA, D., & HUNTSMAN. (2000). Geochemistry and Tectonic Setting of Mafic Igneous Units in the Neoproterozoic Katangan Basin, Central Africa: Implications for Rodinia Break-up.

[30]. KAPENDA , D. (1986). Le plutonisme du Nord-est du Katanga (R.D.C). Thèse. UNILU. Fac. Sciences. Dép. Géol. Tome 1 & 2.Lubumbashi.

[31]. KIPATA, L. (2013). Brittle tectonics in the Lufilian fold-and-thrust belt and its foreland. An insight into the stress field record in relation to moving plates (Katanga, DRC). PhD. Thesis, Geodynamics and Geodfluids Research Group. Leuven, Belgique.

[32]. KOKONYAGI, J., KAMPUNZU, A., AMSTRONG, R., YOSHIDA, M., OKUDAIRI, T., ARIMA, M., & NGULUBE, D. (2006). The Mesoproterozoic kibaride belt (Katanga, SE D.R. Congo). African Earth Sciences, 46.

[33]. LAFLÈCHE, M., DUPUY, C., & BOUGAULT, H. (1992). Geochemistryandpetrogenesisof Archean mafic volcanic rocks of the southemAbitibi Belt Québec.PrecambrianResearch,volume 57. 207-241.

[34]. LEFEBVRE, J. (1973). Présence d'une sédimentation pyroclastique dans le Mwashya inférieur du Shaba méridional. Annale Societé Géologique Belge. Liège,197-217. Liege.

[35]. LEFEBVRE, J. (1985). Le groupe du Mwashya : Mégacyclothème terminal du Roan (Shaba, Zaïre sud-oriental). Volcanisme et dynamique du bassin sédimentaire. Tervuren.

[36]. LEFEBVRE, J., & CAILTEUX, J. (1975). Volcanisme et minéralisation diagénetiques dans le gisement de l'étoile, Shaba. Annale Societe Géologique Belge, 98 :177-195.

[37]. LEFEBVRE J-J (1989a). Depositional environment of copper-cobalt mineralization in the Katangan sediments of southeast Shaba,Zaire. In: Boyle RW, Brown AC, Jefferson CW, Jowett EC,Kirkham RV (eds.) Sediment-hosted stratiform copper deposits.Spec Pap Geol Assoc Can 36:401–426

[38]. LEPERSONNE. (1974). Carte Géologique du Zaïre. Département des Mines, République du Zaire. Musée royal de l'Afrique Centrale, Belgique. p.67.

[39]. LORIS, N.B.T.H., 1996. Etude des minéralisations uranifères du gisement cuprocibaltifère de Lwishishi (Shaba, Zaire): contextes géologiques et géochimiques. Discussions des modèles génétiques. Unpublished Ph.D. Dissertation, Polytechnic faculty of Mons, Belgium, 275 pp.

[40]. MALAISSE, F. (1975). Caractéristique climatique et écologique du Shaba (Zaïre). Annexe de société géologique. Belgique p117-145

[41]. MASHALA, T.P. (2007). Sédiments ferrifères volcanogéniques et roches associées du Mwashya (Néoproterozoique) de la region Likasi-kambove-Mulungwisha (Katanga meridional). Etudes géochimique, petrographique et mineralogique. Signification géodynamique et paléoenvironnementale.Thèse de doct. en Sciences, UNILU, Fac.Sciences, Lubumbashi, 306p.

[42]. MASTER S, RAINAUD C, ARMSTRONG RA, PHILLIPS D, ROBB LJ (2005). Provenance ages of the Neoproterozoic Katanga Supergroup (Central African Copperbelt), with implications for basin evolution. J Afr Earth Sci. 42:41–60

[43]. NGOYI, K., & DEJONGHE, L. (1995). Géologie et genèse du gisement stratoïde cuprifère de Kinsenda (SE du Shaba, Zaïre).Bulletin de la Société belge de géologie, T. 104 (3-4), p.245-281.

[44]. OKITAUDJI, L.R. 1989 : *Géologie sédimentaire et concentration syndiagénétique du cuivre et de cobalt dans la série des mines du Shaba, Zaïre.* Thèse de doctorat Sci. INPL (France). 427p.

[45]. OKITAUDJI, L.R. 1997 **:** L'évolution tectonique des modèles génétiques du cuivre et du cobalt dans l'Arc cuprifère du Shaba et de la Zambie, discussion colloque internationale Cornet (gisement stratiforme de cuivre et minéralisation associée). Acad. Royal. Sciences d'outre-mer, 103- 121pp.
[46]. OOSTERBOSCH R. (1962) : Les relations entre les minéralisations et les structures des roches dans les ore bodies stratiformes du Katanga. In gisements stratiformes de cuivre en Afrique. Symp. 2[e] partie coordonnée de LOMBARD été NICLINI, pp 105-115
[47]. OOSTERBOSCH, R. (1962). Les minéralisations dans le système de Roan au Katanga in Lombard J.et Nicolini P(Ed).Gisement stratiforme de cuivre en Afrique 1 erepartie Assoc.des Serv.Géol. Afr.Paris.
[48]. PEARCE, J., HARRIS, N., & TINDLE, A. (1984). Trace element discrimination diagram for tectonic interpretation.
[49]. PERRIER, C., & AUGERE, B. (2008). géologie tout en un. BCPSP. Paris: Dunod.
[50]. PORADA, H., BERHORST, V., 2000. Towards a new understanding of the Neoproterozoic–Early Palaeozoic Lufilian and northern Zambezi Belts in Zambia and the Democratic Republic of Congo. J. Afr. Earth Sci. 30, 727–771.
[51]. ROBERT, M. (1950). Les cadres de la géologie du Katanga. Extrait des C.R. Congrès Scientifique (Vol. 2). Elisabethville.
[52]. ROBERT, M. (1956). Géologie et Géographie du Katanga.Bruxelles. 620p.
[53]. ROLLINSON, H. (1993). Using geochemical data: evaluation, presentation, interpretation. United Kingdom,: Longman.
[54]. SELLEY D, BROUGHTON D, SCOTT R, HITZMAN M, BULL SW, LARGE RR,MCGOLDRICK PJ, CROAKER M, POLLINGTON N, BARRA F (2005)
[55]. A newlook at the geology of the Zambian Copperbelt. In: Hedenquist JW, Thompson JFH, Goldfarb RJ, Richards JP (eds.) Economic Geology 100[th]Anniversary Volume, p. 965–1000
[56]. THORNTON, C., & TUTTLE, O. (1960). Chemistry of the igneous rocks: part I ; Differentiation index, Amer. J. Sci., 2558,. 664-684.
[57]. TSHIMANGA, K. (1991). Magmatisme Ubendien de la région de Lumono (NE du Shaba, Zaïre). Thèse Doc. Dpt Geol. Université de Lubumbashi, 241p Vol.1. Lubumbashi.
[58]. UNRUG R (1988). Mineralization controls and source of metals in the Lufilian fold belt, Shaba (Zaire), Zambia, and Angola. Econ Geol 83:1247–1258
[59]. VANCUTSEM, C., KIBAMBE LUBAMBA, J.-P., BLAES, J.-F., PEKEL, J.-F., DE WASSEIGE, C., & DEFOURNY, P. (2006). Carte de la République Démocratique du. la – Neuve, Belgique.
[60]. WENDORFF, M. (2000). Revision of the stratigraphical position of the "Roches Argilo-Talqueuses" (RAT) in the Neoproterozoic Katangan Belt, South Congo. African Earth Sciences, 717 - 716.

Mwitwa K.M." Geodynamic Environment and Geochemical Control of Gabbroic Intrusions in Southwest Haut-Katanga in the Kapande Area: (Democratic Republic of Congo)."IOSR Journal of Applied Geology and Geophysics (IOSR-JAGG) 6.6 (2018): 56-71.